Received: 27 March 2024 | Revised: 26 June 2024 | Accepted: 30 June 2024

DOI: 10.1002/cbf.4091

RESEARCH ARTICLE

CELL BIOCHEMISTRY & FUNCTION WILEY

Intron retention in PI-PLC γ1 mRNA as a key mechanism affecting MMP expression in human primary fibroblast-like synovial cells

Alessia Mariano[1] | Sergio Ammendola[2] | Arianna Migliorini[3] | Martina Leopizzi[4] | Domenico Raimondo[3] | Anna Scotto d'Abusco[1]

[1]Department of Biochemical Sciences, Sapienza University of Rome, Roma, Italy

[2]Ambiotec di Sergio Ammendola, Cisterna di Latina, Italy

[3]Department of Molecular Medicine, Sapienza University of Rome, Rome, Italy

[4]Department of Medico-Surgical Sciences and Biotechnologies, Polo Pontino-Sapienza University, Latina, Italy

Correspondence
Anna Scotto d'Abusco, Department of Biochemical Sciences, Sapienza University of Rome, P.le Aldo Moro, 5, 00185 Roma, Italy.
Email: anna.scottodabusco@uniroma1.it

Funding information
Progetto Avvio alla Ricerca 2021, Grant/Award Number: AR12117A2DCE5BF7; Progetto Facoltà 2020, Grant/Award Number: RP1201729DF2A57F

Abstract

The intron retention (IR) is a phenomenon utilized by cells to allow diverse fates at the same mRNA, leading to a different pattern of synthesis of the same protein. In this study, we analyzed the modulation of phosphoinositide-specific phospholipase C (PI-PLC) enzymes by *Harpagophytum procumbens* extract (HPE) in synoviocytes from joins of osteoarthritis (OA) patients. In some samples, the PI-PLC γ1 isoform mature mRNA showed the IR and, in these synoviocytes, the HPE treatment increased the phenomenon. Moreover, we highlighted that as a consequence of IR, a lower amount of PI-PLC γ1 was produced. The decrease of PI-PLC γ1 was associated with the decrease of metalloprotease-3 (MMP-3), and MMP-13, and ADAMTS-5 after HPE treatment. The altered expression of MMPs is a hallmark of the onset and progression of OA, thus substances able to decrease their expression are very desirable. The interesting outcomes of this study are that 35% of analyzed synovial tissues showed the IR phenomenon in the PI-PLC γ1 mRNA and that the HPE treatment increased this phenomenon. For the first time, we found that the decrease of PI-PLC γ1 protein in synoviocytes interferes with MMP production, thus affecting the pathways involved in the MMP expression. This finding was validated by the silencing of PI-PLC γ1 in synoviocytes where the IR phenomenon was not present. Our results shed new light on the biochemical mechanisms involved in the degrading enzyme production in the joint of OA patients, suggesting a new therapeutic target and highlighting the importance of personalized medicine.

KEYWORDS
Harpagophytum procumbens, intron retention, metalloproteases, osteoarthritis, personalysed medicine, phosphatidylinositol-phospholipase C γ1

1 | INTRODUCTION

Intron retention (IR) is one of the forms of alternative splicing, the mechanism that allows to get more protein isoforms from the same gene.[1] For several years, the IR has been considered a misfunctioning of spliceosome machine, for this reason it has been barely considered in mammalian systems.[2] In the last years, several studies showed that IR is one of the mechanisms utilized by cells to allow diverse fates at the same mRNA and consequently at the protein codified by that mRNA.[1] Many introns contain stop codons in frame with the sequence presents in the exon, in this case the IR leads to the production of a mRNA that can be degraded in some ways

resulting in non-expression of that protein.[3–5] Alternatively, the intron-retained transcript can be transported into cytoplasm and transcribed giving proteins with novel biological functions, thus the mechanism is part of regulated gene expression program diffused among living organisms including plants and mammals.[6,7] Recently, a study carried out on 2500 human mRNAs showed that the IR phenomenon is ubiquitous and can affect up to 80% of the transcript,[8] emphasizing its biological significance. To date, increasing body of evidence indicates that regulated IR is involved in cell development, cell differentiation and in response to stress stimuli.[9–11] Prolonged stress stimuli can lead to inflammation which in turn can become chronic giving several types of disease.[12] Impaired splicing machines or aberrant IR have been described to be involved in inflammatory diseases, spanning from rheumatoid arthritis to many kinds of cancers, where it affects the expression of tumor-suppressor genes.[13,14] Our model of study is the osteoarthritis (OA), which is characterized by chronic low-grade inflammation.[15] OA is a degenerative joint disease involving all the components of the joint, synovial membrane, subchondral bone, and cartilage. The inflammatory stimuli start from fibroblast-like synoviocytes (FLSs), one of the two cell types present in the synovial membrane,[16] involving in turn also chondrocytes, where the secretion of specific enzymes play the pivotal role in the homeostasis of extracellular matrix (ECM) components leading to joint cartilage destruction. The chondrocytes, the only cell type present in adult health cartilage, are quiescent and ensure little turnover of the cartilage matrix, whereas, in OA, they are characterized by proliferation activity, cluster formation, and high production of both matrix proteins and matrix-degrading enzymes. All these phenomena lead to inappropriate matrix remodeling, chondrocyte hypertrophy, and cartilage calcification.[17] The matrix-degrading enzymes involved in OA, produced by both chondrocytes and synoviocytes, include, among others, aggrecanases and collagenases, which belong to the metalloprotease (MMP) family.

The progression of OA, alongside the activation of inflammatory pathways, is also characterized by joint pain, and it is treated with analgesic agents, nonsteroidal anti-inflammatory, and painkiller drugs, with the aim to alleviate the symptoms. Nutraceuticals are also used to treat OA, with the dual purpose of delaying cartilage degradation and alleviating the symptoms. Among the most widely used nutraceuticals, compositions containing glucosamine, chondroitin sulfate, and *Harpagophytum procumbens* extract are administered. *H. procumbens* is an ethnomedicinal herb traditionally used for joint pain associated with OA. Previously, we studied the effects of *H. procumbens* extract in human primary synoviocytes isolated from OA patients who underwent prosthesis surgery.[18] Initially, in that study, the synovial tissues were characterized for the presence of cannabinoid receptors, CB1 and CB2, and for phosphoinositide-specific phospholipase C (PI-PLC) isoforms, with the aim to analyze intracellular targets involved in the pain pathways. We compared OA and non-OA synovial tissues, finding that, regarding the PI-PLC β isoforms, they were differentially expressed in those tissues, in particular PI-PLC β2 was more expressed in OA and at lesser degree in non-OA tissues.[18] Moreover, we studied the effectiveness of *H. procumbens* extract to modulate the MMP production, paying particular attention to MMP-13, a collagenase which is considered a hallmark of OA, involved in the degradation of collagen type II, typical of cartilage, finding a good effectiveness of the extract.[19]

In the present manuscript, we analyzed in more depth the expression of all the PI-PLC isoforms in human synoviocytes, and the effects of *H. procumbens* extract treatment on phospholipase expression. Moreover, we go through the IR phenomenon in the PI-PLC γ1 isoform, looking for an association between PI-PLC γ1 and some MMPs, such as MMP-3, -13, and ADAMTS-5 production.

Significant Statement

This manuscript focuses on the modulation of phosphoinositide-specific phospholipase C (PI-PLC) γ1 in human primary fibroblast-like synoviocytes, which leads to the modulation of metalloprotease-3 (MMP-3), MMP-13, and ADAMTS-5, involved in the degradation of extracellular matrix in degenerative joint diseases. We found that in some synoviocyte samples, the PI-PLC γ1 mRNA incurs in the intron retention (IR) phenomenon, which results in an unsuccessful translation of the proteins associated with the decrease of MMP enzymes. Moreover, IR is increased after cell treatment with *Harpagophytum procumbens* extract (HPE), traditionally used to treat osteoarthritis. Considering that HPE results are effective in modulating MMPs only in synoviocyte samples where the IR phenomenon is present, it is necessary to evaluate individual variability in the personalized medicine field.

2 | MATERIALS AND METHODS

2.1 | Human primary cell isolation

Human primary FLSs were isolated from synovial membranes obtained from OA patients that underwent total knee arthroplasty surgery. Full ethical consent was obtained from all donors, and the Research Ethics Committee, ASL Lazio 2 (#005605/2019, March 3, 2019) approved the study. In brief, the synovial membrane fragments were minced and treated with 1 mg/mL collagenase type IV and 0.25% trypsin for 2 h at 37°C in agitation. Then, cells were grown to 80% confluence in Dulbecco's Modified Eagle Medium (DMEM) (HyClone) supplemented with L-glutamine, penicillin/streptomycin (Sigma-Aldrich), and 10% fetal bovine serum (FBS) and cultured at 37°C and 5% CO_2. All experiments were carried out with synoviocytes at first passage (p1), isolated from at least three different donors.

2.2 | Cell treatment

Cells were left untreated (CTL) or treated for required times with 0.1 mg/mL of *Harpagophytum procumbens* extract (HPE) dissolved in DMSO (HPE_{DMSO}). The standardized dried HPE, containing 1.2% harpagoside, was provided by ACEF S.p.a., and the HPE_{DMSO} was previously characterized as reported in Mariano et al.[18] Solvent alone was tested, too. Experiments were independently repeated at least three times.

2.3 | RNA extraction and reverse-transcription

Total RNA was extracted from untreated and treated FLSs, with Blood/Tissues Total RNA extraction kit (Fisher Molecular Biology), and the reverse transcription was performed according to the manufacturers' instructions by OneScript Hot Reverse Transcriptase (Applied Biological Materials Inc.).

2.4 | Semiquantitative-PCR

PCR was used to study the modulation of PI-PLC enzymes in HPE_{DMSO}-treated FLSs in comparison with the untreated ones. PCR reactions were performed with MyTaq DNA Polymerase (Bioline) following manufacturers' instructions. Cycling conditions were performed with a 95°C initial denaturation step for 1 min, followed by 30 cycles consisting of 95°C denaturation (30 s), annealing (30 s) at 56°C and 72°C extension (1 min) in Mastercycler™ (Eppendorf) thermocycler. Primers (Table 1), synthesized by Biofab Research, were designed using Primer Express software v1.4.0 (Applied Biosystems).[20] Amplified PCR products were analyzed by 1.5% agarose gel electrophoresis using Glyceraldehyde 3-phosphate dehydrogenase (GAPDH) as a housekeeping gene. Image acquisitions were performed by ChemiDoc Instrument (Bio-Rad Laboratories).

2.5 | Quantitative-real time-PCR (RT-PCR)

Quantitative RT-PCR analysis was performed using an ABI Prism 7300 (Applied Biosystems; Thermo Fisher Scientific). Amplification was carried out using SensimixPlus SYBR Master mix (Bioline). Primers (Table 2), synthesized by Bio-Fab research, were designed using Primer Express software v1.4.0 (Applied Biosystems). Data were analyzed by $2^{-\Delta\Delta C_t}$ method, determining the transcript abundance relative to 18S housekeeping gene.

2.6 | PCR products sequencing

PCR products, obtained with primers PI-PLC γ1 (Table 1), were purified through the extraction by agarose gel and were sequences by Biofab Research.

TABLE 1 List of primers used for PCR of PI-PLC genes.

Gene	Primer sequences (forward-reverse)
PI-PLC β1 OMIM*607120	5′-AGCTCTCAGAACAAGCCTCCAACA-3′ 5′-ATCATCGTCGTCGTCACTTTCCGT-3′
PI-PLC β2 OMIM *604114	5′-AAGGTGAAGGCCTATCTGAGCCAA-3′ 5′-CTTGGCAAACTTCCCAAAGCGAGT-3′
PI-PLC β3 OMIM *600230	5′-TATCTTCTTGGACCTGCTGACCGT-3′ 5′-TGTGCCCTCATCTGTAGTTGGCTT-3′
PI-PLC β4 OMIM *600810	5′-GCACAGCACACAAAGGAATGGTCA-3′ 5′-CGCATTTCCTTGCTTTCCCTGTCA-3′
PI-PLC γ1 OMIM *172420	5′-TCTACCTGGAGGACCCTGTGAA-3′ 5′-CCAGAAAGAGAGCGTGTAGTCG-3′
PI-PLC γ2 OMIM *600220	5′-AGTACATGCAGATGAATCACGC-3′ 5′-ACCTGAATCCTGATTTGACTGC-3′
PI-PLC δ1 OMIM *602142	5′-CTGAGCGTGTGGTTCCAGC-3′ 5′-CAGGCCCTCGGACTGGT-3′
PI-PLC δ3 OMIM *608795	5′-CCAGAACCACTCTCAGCATCCA-3′ 5′-GCCA TTGTTGAGCACGTAGTCAG-3′
PI-PLC δ4 OMIM *605939	5′-AGACACGTCCCAGTCTGGAACC-3′ 5′-CTGCTTCCTCTTCCTCATATTC-3′
PI-PLC ε OMIM *608414	5′-GGGGCCACGGTCATCCAC-3′ 5′-GGGCCTTCATACCGTCCATCCTC-3′
PI-PLC η1 OMIM *612835	5′-CTTTGGTTCGGTTCCTTGTGTGG-3′ 5′-GGATGCTTCTGTCAGTCCTTCC-3′
PI-PLC η2 OMIM *612836	5′-GAAACTGGCCTCCAAACACTGCCCGC-3′ 5′-GTCTTGTTGGAGATGCACGTGCCCCTT-3′
GAPDH NM_02046	5′-CGAGATCCCTCCAAAATCAA-3′ 5′-GTCTTCTGGGTGGCAGTGAT-3′

Note: The PI-PLC-specific online Mendelian in man (OMIM) numbers are indicated.

Abbreviation: PI-PLC, phosphoinositide-specific phospholipase C.

2.7 | Immunofluorescence analysis

PI-PLC γ1 was visualized by immunofluorescence. Cells, plated at a density of $8 \times 10^3/cm^2$, were left untreated (CTL) or treated with HPE_{DMSO} for the required time. Then, cells were washed in phosphate buffer saline (PBS), fixed in 4% paraformaldehyde in PBS for 15 min at 4°C, and permeabilized with 0.5% Triton-X 100 in PBS for 10 min at room temperature. After blocking with 3% bovine serum albumin in PBS for 30 min at room temperature, cells were incubated at 1 h, at room temperature, with PI-PLC γ1 mouse monoclonal primary antibody (sc-7290, specific for an epitope mapping between amino acids 1243−1262 near the C-terminus of protein; Santa Cruz Biotechnology) diluted 1:50. Cells were washed with PBS and then, incubated for 1 h, at room temperature, with Alexa Fluor 595 (red) donkey anti-rabbit secondary antibody (Invitrogen; Thermo Fisher Scientific) diluted 1:300. Slides were washed and then, stained with DAPI (Invitrogen; Thermo Fisher Scientific) to visualize the nuclei in blue. The images were captured by a Leica DM IL LED optical microscope using an AF6000 modular microscope (Leica Microsystem).

TABLE 2 List of primers used for RT-PCR.

Gene	Primer sequences (forward-reverse)
MMP-3 NM_002422.5	5′-CCTGGTACCCACGGAACCT-3′ 5′-AGGACAAAGCAGGATCACAGTT-3′
MMP-13 NM_002427	5′-TTCTTGTTGCTGCGCATGA-3′ 5′-TGCTCCAGGGTCCTTGGA-3′
ADAMTS-5 NM_007038.5	5′-GCACTTCAGCCACCATCAC-3′ 5′-AGGCGAGCACAGACATCC-3′
PI-PLC γ1 NM_182811.2	5′-CTACCTGGAGGACCCTGTGAAC-3′ 5′-ATCCTCGTTGCCCTGGTCACTG-3′
PI-PLC γ1 (204) DQ297143.1	5′-GCCATGTGCCATCTCTATTG-3′ 5′-CATAAACAGACTCCAACGGC-3′
PI-PLC γ1 (205) DQ297143.1	5′-AGCCTGTCCCACAGGTCAG-3′ 5′-CTGAGAACAGGCAGAGTCAG-3′
PI-PLC γ1 (207) DQ297143.1	5′-CAAGGACCTGAGAACATGC-3′ 5′-GGCAGTCAGATCTTAAGAGG-3′
PI-PLC γ1 (208) DQ297143.1	5′-TGACCATTGGTGGGCTTTG-3′ 5′-AATCTGACAAGCCGGCACAT-3′
PI-PLC γ1 (212) DQ297143.1	5′-AGCTTTGCCGAGTGTCCCTTC-3′ 5′-CAATGTCAGCCCAGCCATAC-3′
18S NM_003286	5′-CGCCGCTAGAGGTGAAATTC-3′ 5′-CATTCTTGGCAAATGCTTTCG-3′

Note: The Accession Numbers are indicated. Regarding the primer pairs used to amplify PI-PLC 1 204, 205, 207, 208, and 212, they are formed by one oligonucleotide mapping inside an exon and the other one mapping in an intron.

Abbreviation: PI-PLC, phosphoinositide-specific phospholipase C.

TABLE 3 Annealed siRNA sequences.

siRNA	Sequence
$siRNA_{360}$	5′-GGGACUUUGAUCGCUAUCATT-3′ 5′ -UGAUAGCGAUCAAAGUCCCTT-3′
$siRNA_{3665}$	5′-GUGCCUUUGAAGAACAACUTT -3′ 5′-AGUUGUUCUUCAAAGGCACTT-3′
$siRNA_{1520}$	5′-GUGCCUACAUCCAUGAUGUTT-3′ 5′-ACAUCAUGGAUGUAGGCACTT-3′
$siRNA_{1635}$	5′-CCAGCAGCAAGAUCUACUATT -3′ 5′-UAGUAGAUCUUGCUGCUGGTT-3′
NC	5′-UUCUCCGAACGUGUCACGUTT-3′ 5′-ACGUGACACGUUCGGAGAATT-3′
PC_GAPDH	5′-UGACCUCAACUACAUGGUUTT-3′ 5′-AACCAUGUAGUUGAGGUCATT-3′

2.8 | Protein 3D modeling and aggregation propensity prediction

The structure models of PI-PLC γ1 was generated using AlphaFold2 and the results visualized in ChimeraX.[21,22] AGGRESCAN3D v. 2.0 was used to determine the aggression propensity of translated protein with retained intron.[23]

2.9 | MMP-3, MMP-13, and ADAMTS-5 ELISA assay

The amount of MMP-3, MMP-13, and ADAMTS-5 proteins in the cell supernatant was determined using an ELISA kit (Fine Test ELISA; Fine Biotech Co., Ltd.) according to the manufacturer's instructions. Optical density (OD) absorbance was measured at 450 nm by a microplate reader (NB-12-0035; NeBiotech).

2.10 | siRNA transfections

Four different siRNA oligos targeting PI-PLC γ1 (Table 3), negative control (NC), and positive control (PC) siRNA (GAPDH) were designed by GenePharma (Zhangjiang Hi-Tech Park). All four annealed siRNAs, NC and PC, were transfected in human primary FLSs in 24-well plates using DreamFect Gold (OzBiosciences). Briefly, 50 nM final concentration of each siRNA was diluted in Opti-MEM (Gibco, Cat. 31,985,062), followed by the addition of 5 μL/sample of DreamFect Gold (Cat. DG80500). After an incubation of 15 min, the mix was added to 7.5×10^4 cells/0.5 mL in each well in DMEM supplemented with 10% FBS and allowed to grow 24, 48, and 72 h at 37°C in a CO_2 incubator. To verify the effectiveness of silencing, transfected cells with the four siRNA oligos were analyzed by RT-PCR and immunofluorescence for PI-PLC 1 γ1.

2.11 | Statistical analysis

All data were obtained from at least three independent experiments, each performed either in duplicate or in triplicate. Data were statistically analyzed with two-way repeated measures analysis of variance with Bonferroni's multiple comparison test, using Prism 5.0 software (GraphPad Software). $p < .05$ was considered significant.

3 | RESULTS

3.1 | Differential expression of PI-PLC isoforms in synovial cells with and without HPE treatment

Previously, in our laboratory, we found that some PI-PLC isoforms were differently expressed in synovial tissue from OA and NON-OA patients.[18] In particular, the PI-PLC β2 was expressed on synovial membranes from OA patients and was almost no detectable in NON-OA patients. Moreover, the expression of PI-PLC β2 was decreased in FLSs treated with HPE_{DMSO}. To analyze the mRNA expression pattern of all types of PI-PLC after HPE_{DMSO} treatment, a PCR assay was performed, finding that the expression PI-PLC β1 was not

affected by treatment, whereas the expression of PI-PLC β3 and PI-PLC β4 was upregulated, and we confirmed that the expression of PI-PLC β2 was inhibited, even if the modulation was not statistically significant (Figure 1). Regarding the other isoforms of PI-PLC, they were not affected by HPE_{DMSO} treatment, and the PI-PLC δ4 was not detected in this kind of cells (Figure 1). The finding that caught our attention was the presence of two PCR products regarding the PI-PLC γ1 and even more the increase of the second PCR product in the HPE_{DMSO} treated sample (Figure 1). The PCR primers, to amplify PI-PLC γ1, were designed to obtain a PCR product 300 bp long, with the forward and reverse primers mapping inside two different exons (Table 1). In the analyzed samples we found two PCR products, the first one was 300 bp long, and the second one was 500 bp (Figure 1).

To confirm this result, we analyzed PI-PLC γ1 mRNA level in FLSs isolated by 16 patients by PCR assay finding the presence of a double PCR band in about 35% of the analyzed samples, two representative samples both with single and double band are reported in Figure 2A. To understand what the 500 bp long PCR product represented, it was sequenced, finding that it overlapped PI-PLC γ1 complete coding sequence, containing both exons and introns mapping in analyzed region (NCBI accession number: DQ297143.1) (Figure 2B). This result suggests that the splicing process is partially inhibited in those samples having the double band and that the HPE_{DMSO} treatment further inhibits mRNA maturation in the same samples.

3.2 | IR in synovial cells

A genomic analysis regarding the gene encoding for PI-PCL γ1 was conducted by Human and Vertebrate Analysis and Annotation (HAVANA) group at the Wellcome Trust Sanger Institute, whose results are deposited on the ENSAMBLE database (ENSG00000124181). In this analysis, the authors described the retention of some introns in the mature mRNA of PI-PLC γ1, specifically 17 introns in five different regions, named PLCG1-212, PLCG1-207, PLCG1-205, PLCG1-208, and PLCG1-204 (Figure 3A). These regions, depicted in blue in Figure 3A, and magnified in the lower panel, contain both introns (in orange) and exons (in blue). The orange-colored introns indicate those that are retained. Our 500 bp PCR product corresponded to the PLCG1-207 region (Figure 3A and Supporting Information S1: 1).

To verify whether our results showed the same characteristic of the IR described by the HAVANA group, we analyzed our samples by real time-PCR using primer pairs formed by an oligonucleotide mapping in an exon and the other one in an intron of the five regions (Table 2) both on untreated and HPE_{DMSO} treated cells. This approach offers the dual advantage of selectively amplifying samples with retained introns and providing a quantitative measure of PCR products. In samples where splicing occurred correctly, no amplification was observed, whereas the PCR products were obtained in the

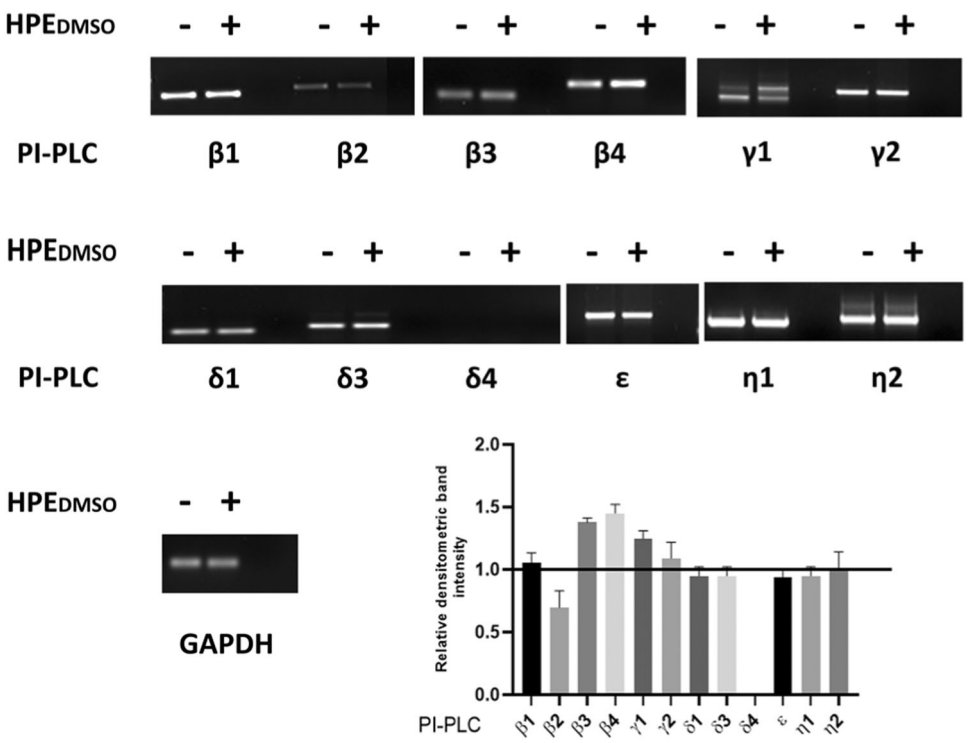

FIGURE 1 PI-PLC isoform expressions after HPE_{DMSO} treatment. Cells were left untreated (−) or treated with 0.1 mg/mL HPE_{DMSO} for 24 h (+), then the mRNA was extracted and analyzed by semiquantitative-PCR. All PI-PLC mRNA levels were reported as relative mRNA expression levels with respect to GAPDH, used as a housekeeping gene. The densitometric analysis (bottom right) was performed by ImageJ. PI-PLC expression of treated samples was normalized to the untreated cells, reported as 1, and represented by a horizontal line. Results are expressed as mean ± SD of data obtained by three independent experiments. HPE, *Harpagophytum procumbens* extract; PI-PLC, phosphoinositide-specific phospholipase C.

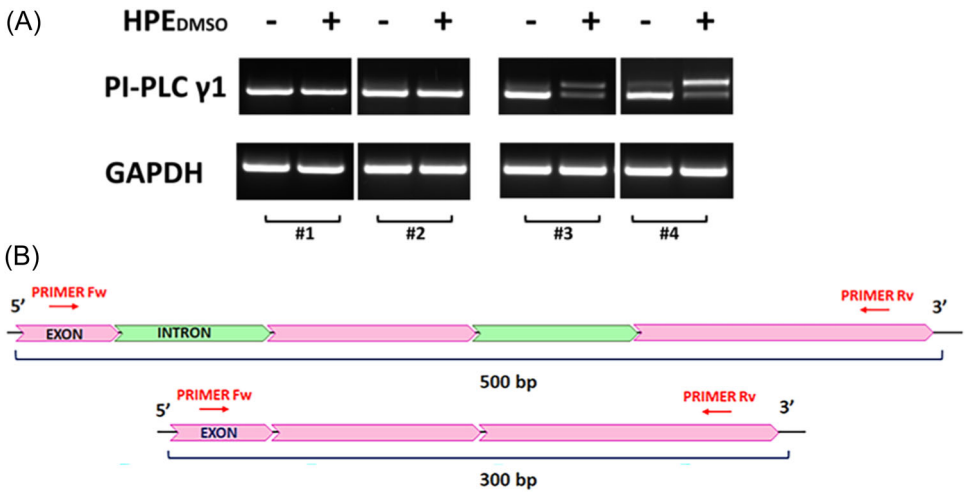

FIGURE 2 PI-PLC γ1 expression after HPE_{DMSO} treatment. (A) Cells were left untreated (−) or treated with 0.1 mg/mL HPE_{DMSO} for 24 h (+), and then the mRNA was extracted and analyzed by semiquantitative-PCR. PI-PLC γ1 mRNA level was reported as a relative mRNA expression level with respect to GAPDH, used as a housekeeping gene. Two representative samples with single bands (left, #1, #2) and two representative samples with double bands (right, #3, #4) are reported. (B) Schematic representation of the region containing the two PCR products obtained from PI-PLC γ1 analysis and confirmed by sequencing. HPE, *Harpagophytum procumbens* extract; PI-PLC, phosphoinositide-specific phospholipase C.

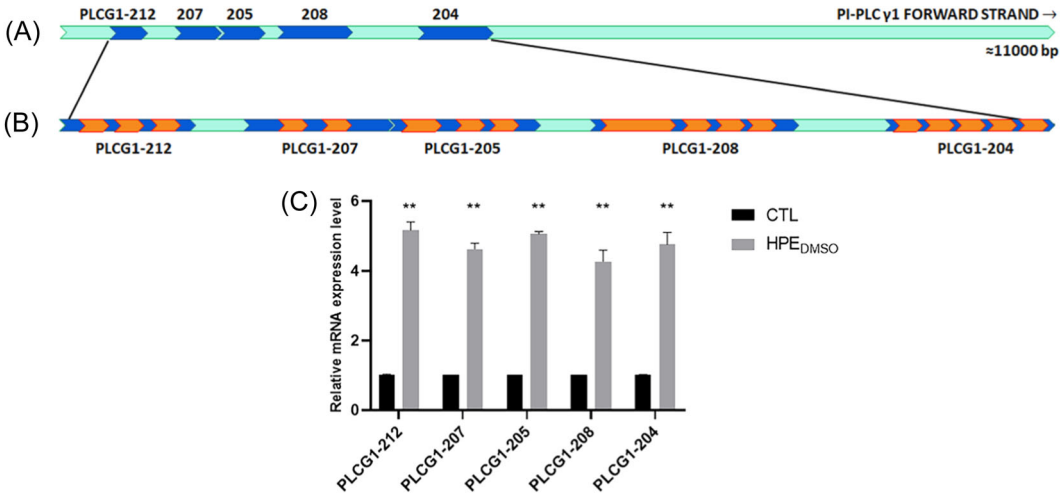

FIGURE 3 (A) Schematic representation of the PI-PLC γ1 coding gene (~11,000 bp) in mint green. Five regions, in blue, of the PI-PLC γ1 gene sequence, containing both introns and exons, showed retained introns, in orange. (B) Magnification of the five regions, exons are depicted in blue, introns in orange. (C) Effects of HPE_{DMSO} on PI-PLC γ1 intron retention. Cells were left untreated (CTL) or treated with 0.1 mg/mL HPE_{DMSO} for 24 h, and then mRNA was extracted and analyzed by real time-PCR. PLCG1-212, 207, 205, 208, and 204 mRNA levels were reported as relative mRNA expression levels with respect to 18S mRNA ($2^{-\Delta\Delta C_t}$ method). Results are expressed as mean ± SD of data obtained by three independent experiments. $^{**}p < .01$ versus CTL. HPE, *Harpagophytum procumbens* extract; PI-PLC, phosphoinositide-specific phospholipase C.

samples retaining introns. Moreover, upon treatment with HPE_{DMSO}, intron-retained PCR products were approximately five times more abundant than those in untreated samples (CTL) (Figure 3B). Furthermore, we found that the samples that retained introns in the PLCG207 region retained introns also in the other four regions, PLCG1-212, PLCG1-205, PLCG1-208, and PLCG1-204, and the treatment with HPE_{DMSO} further enhanced these retentions (Figure 3B and Supporting Information S1: 2).

The sequence analyses showed that stop codons were present inside the retained introns, thus this phenomenon must cause a decrease in the PI-PLC γ1 protein level. To this aim, we analyzed the PI-PLC γ1 protein expression by immunofluorescence experiment, comparing treated and untreated cells showing both single (correct splicing) and double band (retained introns). Notably, the cells before HPE_{DMSO} treatment (CTL) with retained introns showed a lower amount of PI-PLC γ1 protein compared to the cells before HPE_{DMSO}

treatment (CTL), where correct splicing occurred (Figure 4). Following HPE_{DMSO} treatment, cells with retained introns (double band) showed a significant decrease in protein level (Figure 4), while HPE_{DMSO} treated cells with a single band did not show a decrease in the PI-PLC γ1 protein level (Figure 4).

3.3 | PI-PLC γ1 protein 3D modeling and aggregation propensity prediction

To explain what was experimentally observed, we performed a computational analysis of this protein. The mature wild type of PI-PLC γ1 shows distinct patterns of catalytic and regulatory domains as schematized in Figure 5A with corresponding domain-colored surfaces and cartoon model. PI-PLC γ1 possesses a N-terminal Pleckstrin (PH), a helix-loop-helix (EF), a TIM barrel (X box), a split PH (sPH), a N-terminal and C-terminal src homology 2 (nSH2 and cSH2), a SH3, another TIM barrel (Y box), and a C-terminal (C2) domains.[24] The catalytic core comprises an EF-hand, the X-box, the Y-box, and the C2 domains (Figure 5A). The X-region forms one-half of the TIM-barrel-like structure, while the Y-domain forms the other half. PI-PLC γ1 contains a unique region that divides the X and Y domains.[25] This region, corresponding to the regulatory domains, contains split PH domains at the ends (sPH), with the middle portion consisting of two N-terminal Src homology 2 (SH2) domains followed by an SH3 domain.[24]

The IR of the five different regions starts with the retention of the intron in PLCG1-212, which results in adding 30 more amino acids (Figure 5B, in light green) that are specified by intron sequence, followed by a stop codon that leads to a truncated protein (Figure 5B). Due to the presence of a stop codon, as a consequence of IR, at the end of the EF region (RI in Figure 5B), the expressed protein contains only the PH and EF domains, lacking the X-box TIM barrel, sPH, nSH2, cSH2, SH3, Y-box TIM barrel, and C2 domains (Figure 5B). Because this truncated protein lacks the regulatory domain, it is completely inactive. Additionally, we investigated the behavior of this translated intron and analyzed the aggregation propensity of this region. Results from Aggrescan3D showed that aggregation-prone residues with A3D score >0, depicted in red on the plot and in the structure, mainly correspond to the translated intron, which exhibits a high tendency to aggregate (Figure 5C).[23] Taken together, these findings indicate that the addition of 30 amino acids, specified by an intron sequence followed by a stop codon, results in the production of a truncated protein that is completely inactive and has a high tendency to aggregate.

3.4 | The PI-PLC γ1 decrease is correlated to MMP downregulation

In OA, the modulation of MMPs is a mechanism particularly involved in the onset and progression of this disease, for this reason we investigated whether HPE_{DMSO} could modulate their

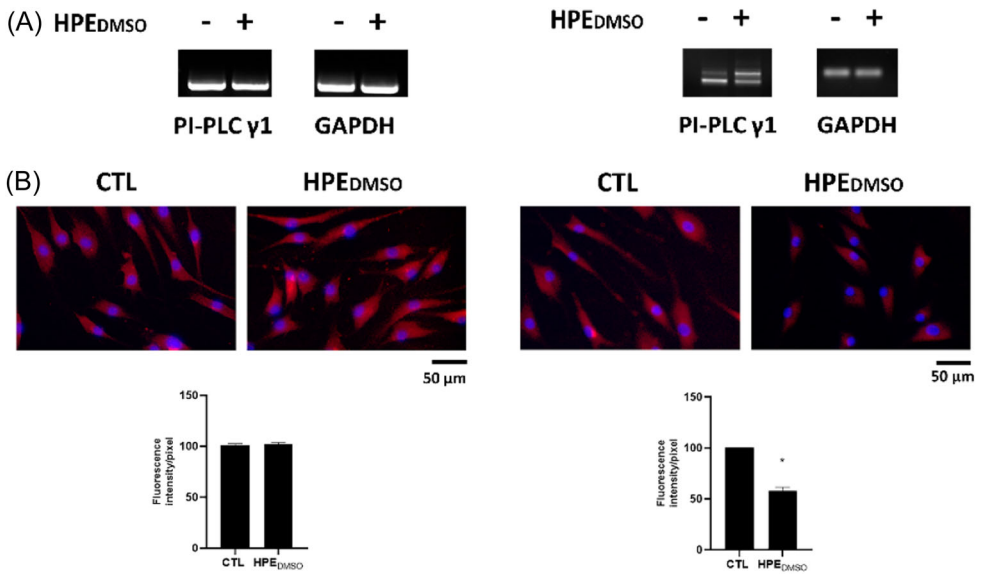

FIGURE 4 PI-PLC γ1 expression in cells with single band (correct splicing, no intron retention [IR]) and double band (IR) before (CTL) and after HPE_{DMSO} treatment. (A) Cells were left untreated (−) or treated with 0.1 mg/mL HPE_{DMSO} for 24 h (+), and then the mRNA was extracted and analyzed by semiquantitative-PCR. PI-PLC γ1 mRNA amount was normalized with respect to the GAPDH housekeeping gene. Regarding the sample with a single band, the showed PCR products are the same as reported in Figure 2A, #1. Regarding the sample with the double band, the showed PCR products are the same as reported in Figure 1 (γ 1 and GAPDH). (B) Human primary FLSs from the sample with no intron retained (left) and with intron retained (right) were stained with anti-PI-PLC γ1 primary antibody and with Alexa Fluor 568 (red) secondary antibody. Nuclei were stained with DAPI (original magnification ×20). The graph represents the pixel intensities in the region of interest obtained by ImageJ. *$p < .05$ versus CTL. FLS, fibroblast-like synoviocytes; HPE, *Harpagophytum procumbens* extract.

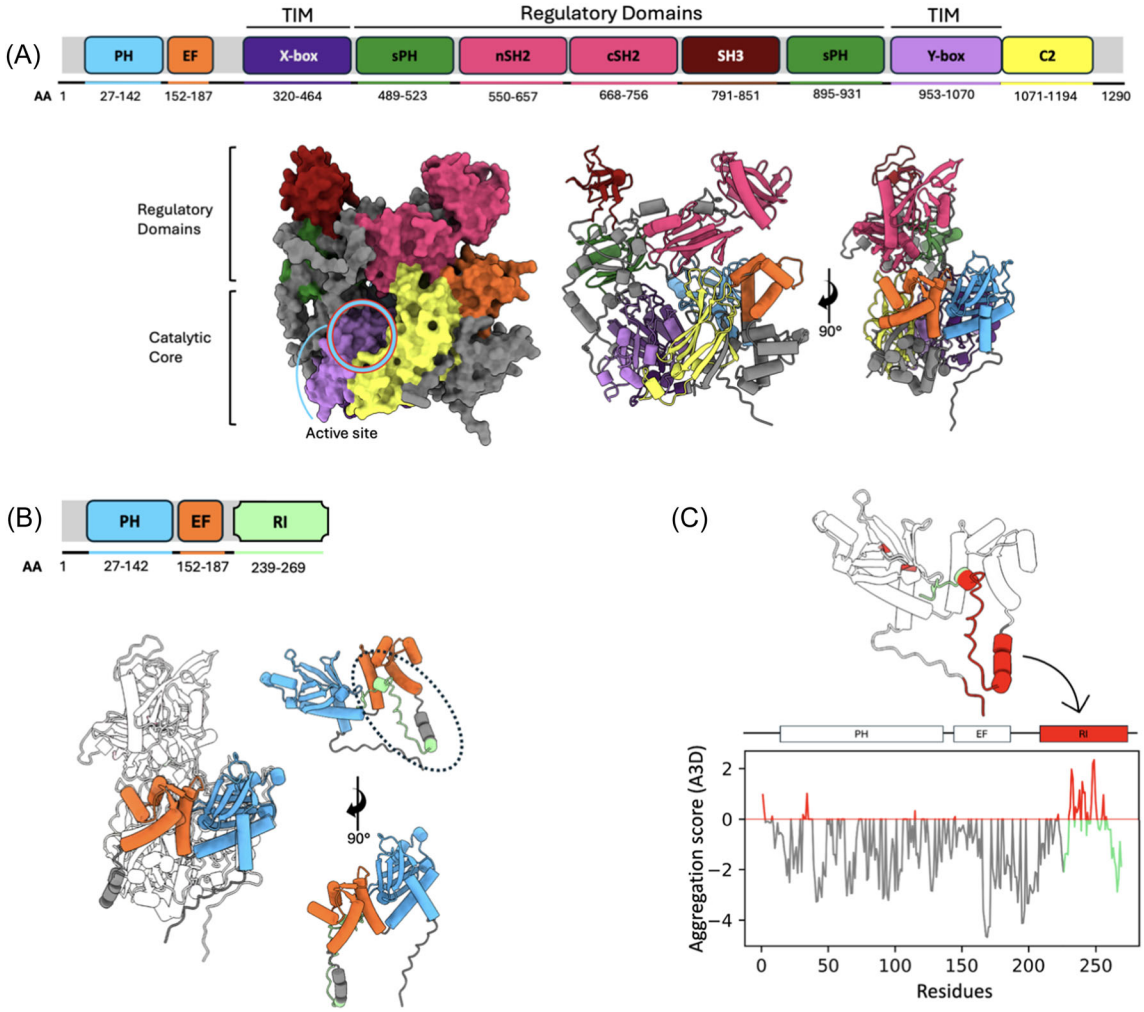

FIGURE 5 Schematic representation of PI-PLC γ1 protein. (A) The distinct patterns of catalytic and regulatory domains with corresponding domain-colored surfaces and a cartoon model of PI-PLC γ1. The catalytic core comprises a helix-loop-helix (EF)-hand, the X-box, the Y-box, and the C-terminal (C2) domains. The X-region forms one-half of the TIM-barrel-like structure, while the Y-domain forms the other half. PI-PLC γ1 contains a unique region that divides the X and Y domains. This region, corresponding to the regulatory domains, contains Pleckstrin (PH) domains at the ends split Pleckstrin (sPH), with the middle portion consisting of two N-terminal Src homology 2 (nSH2 and cSH2) domains followed by an SH3 domain. (B) The intron retention in PLCG1-212 results in the addition of 30 extra amino acids depicted in light green. These amino acids are specified by the intron sequence and are followed by a stop codon, leading to the production of a truncated protein. The resulting expressed protein retains only the N-terminal PH domain and EF-hand domain while losing the remainder of the catalytic core and all the regulatory domains. (C) Aggregation propensity of the protein results from the translation of the retained introns (depicted in light green). The aggregation-prone residues, depicted in red, correspond to an A3D score >0. The entire translated intron exhibits a high tendency to aggregate. RI, retained intron.

expression. During our initial analyses, we found inconsistent results, in some samples, the HPE_{DMSO} treatment was able to induce the decrease of MMP-3, MMP-13, and ADAMTS-5, whereas in cells isolated from other human samples, it was not able to. Considering the IR in the PI-PLC γ1 mRNA and, in turn, in the protein expression downregulation, we explored the possibility that the inconsistent results could be due to normal/abnormal PI-PLC γ1 expression. We treated cells isolated from both kinds of samples, with IR (Figure 6, right side) and correct splicing (Figure 6, left side), finding that HPE_{DMSO} was able to modulate MMPs expression only in cells with PI-PLC γ1 IR and thus a decreased expression of PI-PLC γ1 protein (Figure 6).

3.5 | PI-PLC γ1 silencing in synovial cells with normal splicing

To confirm that the effects of HPE_{DMSO} on the MMP production were correlated to PI-PLC γ1 decreased expression, we silenced PI-PLC γ1 in FLSs that did not show the IR. The effectiveness of PI-PLC γ1 silencing was initially validated by analyzing PI-PLC γ1 mRNA expression after 24 h treatment (Supporting Information S1: Figure 3). As shown in Supporting Information S1: Figure 3, all four siRNA silenced the PI-PLC γ1 mRNA, even if the $siRNA_{3665}$ and $siRNA_{1520}$ were more effective than the other two. Then, we also analyzed the PI-PLC γ1 protein, finding that, after 24-h-treatment, PI-

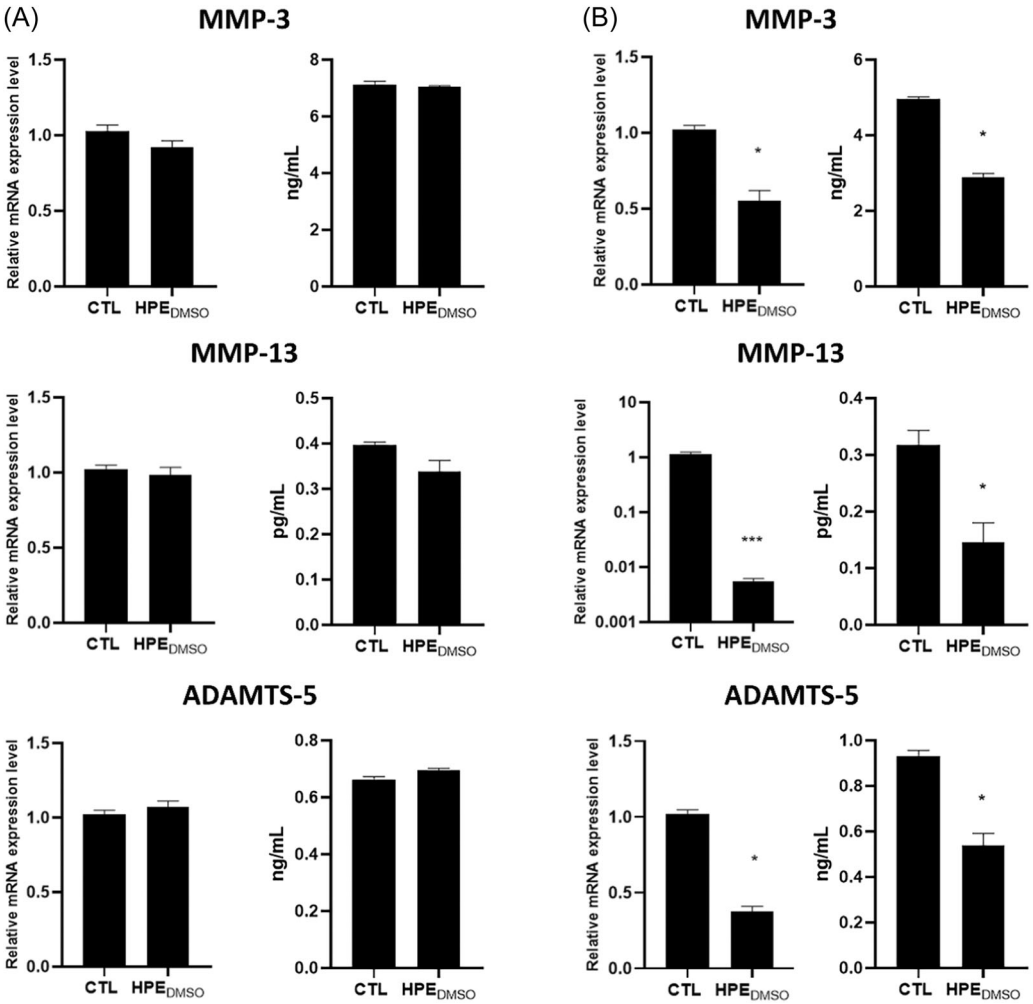

FIGURE 6 Effects of HPE_{DMSO} on the production of MMP enzymes in FLSs showing normal splicing (A) or intron retention (B). Cells were left untreated (CTL) or treated with 0.1 mg/mL HPE_{DMSO} for 24 h (HPE_{DMSO}), and then the mRNA was extracted and analyzed by RT-PCR. MMP mRNA amount was normalized with respect to 18 S ($2^{-\Delta\Delta C_t}$ method, A and B, left columns). Cell culture medium was analyzed by ELISA to measure the secreted MMPs (A and B, right columns). Results are expressed as mean ± SD of data obtained by three independent experiments. *$p < .05$ HPE_{DMSO} versus CTL; ***$p < .005$ HPE_{DMSO} versus CTL. FLS, fibroblast-like synoviocytes; HPE, *Harpagophytum procumbens* extract; MMP, metalloproteases.

PLC γ1 was barely decreased (Supporting Information S1: 4) using all four oligos, whereas, after 48- and 72-h-treatment, the PI-PLC γ1 was strongly decreased (Supporting Information S1: Figures 5 and 6). The $siRNA_{3665}$ and $siRNA_{1520}$ were the most effective, even at the protein level. For the following experiments, $siRNA_{1520}$ was used. In Figure 7, the complete analysis of silenced PI-PLC γ1 with $siRNA_{1520}$ is shown. At the mRNA level, the PI-PLC γ1 decrease was observed at all analyzed times, 24, 48, and 72 h, whereas the PI-PLC γ1 protein level was significantly decreased after 48- and 72-h-silencing (Figure 7).

3.6 | MMP decreasing in PI-PLC γ1-silenced synovial cells

The $siRNA_{1520}$ PI-PLC γ1-silenced cells showed a decrease of MMP-3, -13, and ADAMTS-5 at mRNA and protein levels 48 and 72 h after silencing. These results confirm the correlation between PI-PLC γ1 decrease and MMP modulation (Figure 8), as shown above in cells with IR treated with HPE_{DMSO}.

4 | DISCUSSION

Phospholipase C is expressed in mammals' cells as 13 family members, which preferentially hydrolyze the membrane phospholipid phosphatidylinositol 4,5-bisphosphate, generating two-second messengers, diacylglycerol (DAG) and inositol 1,4,5-triphosphate (IP_3).[26] DAG is retained inside the membrane, where it recruits several factors, including the Protein kinase C, whereas IP_3 diffuses throughout the cytoplasm and interacts with its receptors, leading to Ca^{++} mobilization. Among the 13 isoforms, the PI-PLC-γ is a protein broadly distributed among phylogenetic kingdoms and

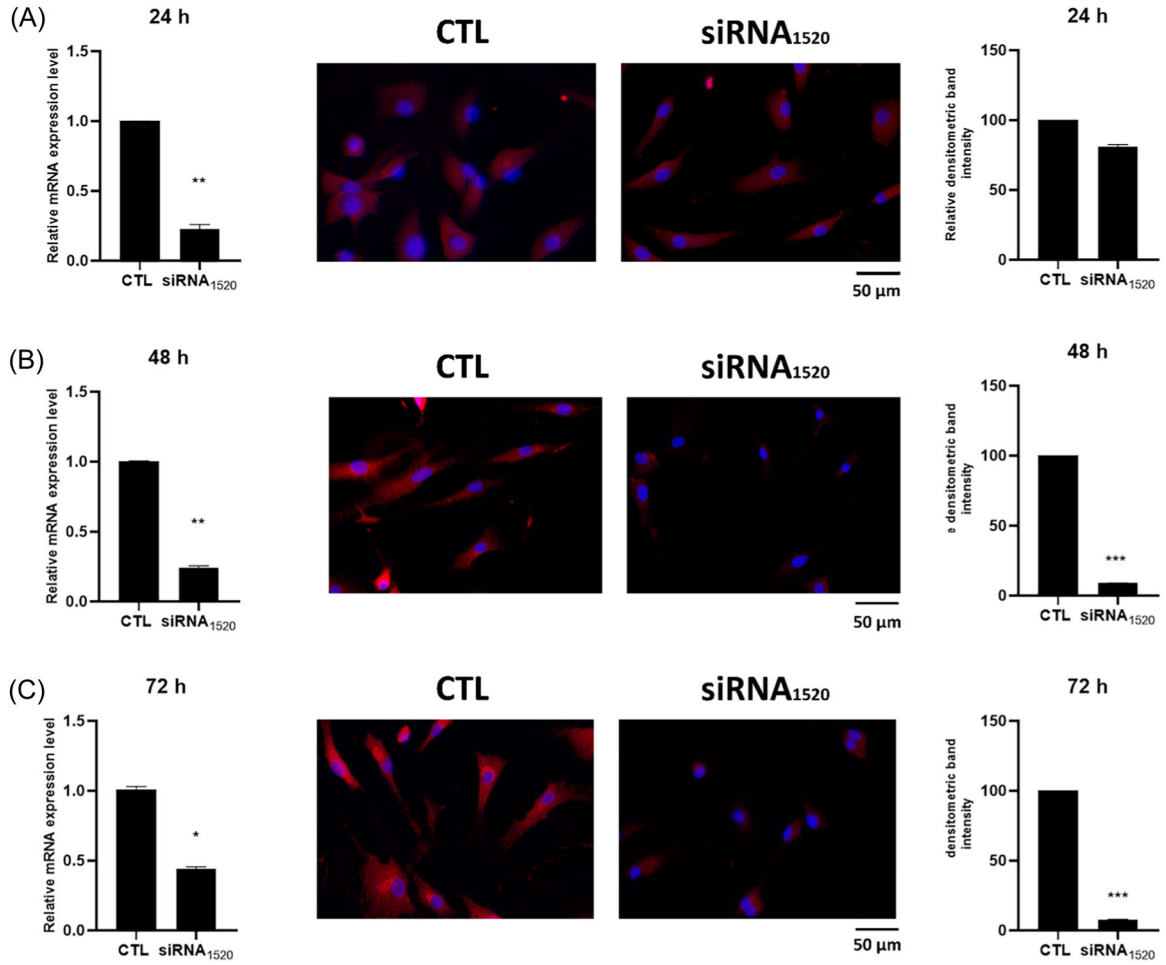

FIGURE 7 PI-PLC γ1 expression in cell silenced with siRNA$_{1520}$ probe. Cells were left non-silenced (CTL) or silenced with siRNA$_{1520}$ for 24 h (A, left column), 48 h (B, left column), and 72 h (C, left column), and then the mRNA was extracted and analyzed by RT-PCR. PI-PLC γ1 mRNA amount was normalized with respect to the 18S housekeeping gene ($2^{-\Delta\Delta C_t}$ method). The PI-PLC γ1-silenced FLSs were stained with anti-PI-PLC γ1 primary antibody and with Alexa Fluor 568 (red) secondary antibody. Nuclei were stained with DAPI (original magnification ×20) for 24 (A), 48 (B), and 72 h (C). On the right, the bar graphs representing the pixel intensities in the region of interest obtained by ImageJ were reported. ***$p < .005$ siRNA$_{1520}$ versus CTL (non-silenced). FLS, fibroblast-like synoviocytes.

mediates the signaling of hormones, growth factors, and other stimuli throughout the consequential activation of inositol lipid signaling pathways.[27] The PI-PLC-γ exists in two main isoforms the γ1, ubiquitously expressed, and the γ2 which is mostly expressed in the cells of the haematopoietic system.[28] The protein structure of PI-PLC γ1, as reported in Section 3, possesses a N-terminal PH, a EF, a TIM barrel X box, a sPH, a nSH2 and cSH2, a SH3, another TIM barrel Y box, and a C2 domains.[24] The PH, EF, the two TIMs (X and Y boxes), and C2 domains represent the enzymatic core, whereas sPH, nSH2, cSH2, and SH3 represent the regulatory domain, which autoinhibits the phospholipase activity. The regulation of two PI-PLC γ expression and their activation are fine-tuned, the PI-PLC γ are activated by a unique mechanism, based on the interaction with receptor and non-receptor tyrosine kinases.[24] The phosphorylation of Tyr783 and Tyr759 sites on PI-PLC γ1 and γ2, respectively, localized inside the X and Y boxes, stimulated their phospholipase activity. In the absence of stimulation, the regulatory domain, which is localized atop the catalytic core, prevents the interaction among enzymes and lipids to be hydrolyzed, thus inhibiting the phospholipase activity.[29]

The human PLCG1 coding gene has been studied and annotated by the HAVANA group. It is a 52,108 bp long gene, producing 23 transcript (splicing) variants, and contains five regions that are involved in the IR phenomenon.[30] These regions, named PLCG1-212, PLCG1-207, PLCG1-205, PLCG1-208, and PLCG1-204, can show irregular splicing leading to the retention of introns. They have stop codons in frame with the exon coding sequence, causing the decrease of PI-PLC γ1 production. In the present study, we found the IR phenomenon in about 35% of the analyzed synovial cells, where it was associated with the decrease of PI-PLC γ1 production. The dysregulation of PI-PLC γ1 has been associated with several pathologies; its increased activity enhanced nuclear factor-κB and interferon type II pathways in monocytes,[31] as well as in T-cell lymphoma and angiosarcoma.[32–34] The IR that we describe does not impair the activation of PI-PLC γ1 but leads to a decrease in protein

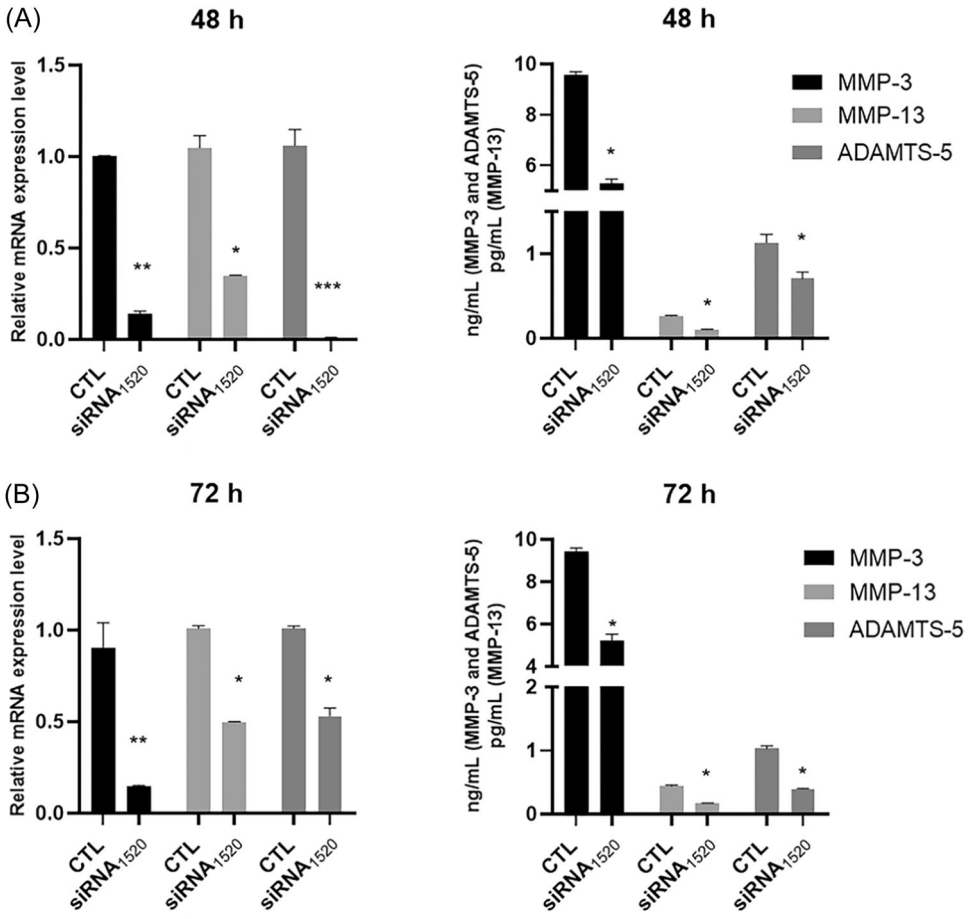

FIGURE 8 Effects of HPE_{DMSO} on the production of MMP enzymes in PI-PLC γ1-silenced FLSs with normal splicing. Cells were analyzed after 48 (A) and 72 h (B) silencing. The mRNA was extracted and analyzed by RT-PCR. MMP mRNA amount was normalized with respect to 18S ($2^{-\Delta\Delta C_t}$ method, left columns). The cell culture medium was analyzed by ELISA to measure the secreted MMPs (right columns). Results are expressed as mean ± SD of data obtained by three independent experiments. *$p < .05$ silenced versus CTL (non-silenced); **$p < .01$ silenced versus CTL; ***$p < .005$ silenced versus CTL. FLS, fibroblast-like synoviocytes; HPE, *Harpagophytum procumbens* extract; MMP, metalloproteases.

production, which, overall, means a smaller amount of active enzyme. The first of five regions, PLCG1-212 that shows the IR, maps within the PI-PLC γ1 coding gene corresponding to the end of the EF region. The retention of introns in PLCG1-212 results in adding 30 more amino acids, which are specified by intron sequence, followed by a stop codon that leads to a nonfunctional truncated protein that exhibits a high aggregation tendency. Anyway, considering that the IR does not affect 100% of the PI-PLC γ1 mRNA, a certain amount of protein is still expressed. The immunofluorescence experiments, using an anti-PI-PLC γ1 antibody, recognizing an epitope mapping at the C-terminal of the protein, show a significant decrease of PI-PLC γ1. The decreased of this protein seems desirable in OA, previously has been described that the inhibition of PI-PLC γ1 stimulates the production of ECM in rat chondrocytes challenged with proinflammatory cytokine IL-1β.[35] Moreover, the intra-articular injection of PI-PLC γ1 inhibitor in rat OA joint showed a decrease of PI-PLC γ1 phosphorylation level, giving a protective action on chondrocytes.[36] In our context, the decreased amount of protein means a lower amount of active PI-PLC γ1 enzyme, which results in a protective action in OA. Intriguingly, the treatment of synovial cells with *H. procumbens* extract further promotes the IR phenomenon, thus leading to a greater decrease of PI-PLC γ1 protein. To date, the OA treatment includes a combination of anti-inflammatory drugs to counteract the symptoms, and nutraceuticals with anti-nociceptive, anti-inflammatory activity and to stimulate the production of ECM components.[37–39] In the last years, in our lab, we studied the *H. procumbens* extract for its action as painkiller and anti-inflammatory agent, finding that the anti-nociceptive action is due to its ability to stimulate the endocannabinoid receptor 2 (CB2) on the plasmatic membrane of synovial cells, which is barely expressed in OA tissues, and to decrease the expression of PI-PLC β2, which is highly expressed in OA tissues.[18] Moreover, the HPE also showed an anti-inflammatory activity downregulating the cAMP and the activation of Protein Kinase A and inhibiting the extracellular signal-regulated kinases (ERK) affecting in turn the expression of MMP-13, which is a hallmark of OA.[19] These results prompted us to go

more in-depth in the study of the effects of HPE on the modulation of all PI-PLC isoforms and MMPs, finding that HPE was able to amply the IR phenomenon and, in certain samples, to modulate the expression of MMP-3, MMP-13, and ADAMTS-5. The observation that HPE was not able to modulate the MMP expression in all analyzed samples suggested us to verify whether there was an association between the PI-PLC γ1 IR and the MMP modulation, finding that the modulation of MMPs was induced by HPE only in those sample that showed the IR in PI-PLC γ1 mRNA. To further demonstrate the association between the decreased expression of PI-PLC γ1 and the modulation of MMPs, we silenced the PI-PLC γ1 mRNA in a sample with normal splicing, confirming, after silencing, the modulation of the MMPs. MMP enzymes are normally expressed in healthy cartilage to allow ECM remodeling, however, in OA, under inflammatory stimulation, the MMP-3, -13, and ADAMTS-5 levels increase causing the onset and progression of the disease.[40–42] The MMP-3, also named stromelysin-1, hydrolyzes some ECM components, such as fibronectin, gelatin, a core protein of proteoglycans, laminin[43,44]; the MMP-13 hydrolyzes the collagen type II, the most represented type in cartilage[45]; and finally, ADAMTS-5 is the major aggrecan-degrading enzymes, which is the component of articular cartilage able to support compressive loads,[46–49] and, in the last years, it has been regarded as a potentially target for OA treatment.[50] The MMP mRNA transcription is differently regulated, depending on what kind of stimulus cells undergo.[51] The proinflammatory stimuli, such as those of the cytokines IL-1β, TNF-α, and IL-6, can induce the production of MMPs through the activation of AP-1 and NF-κB transcription factors. In the promoter region of the gene coding for ADAMTS-5, three binding motifs for NF-κB have been found.[52] Previously, the upregulation of PI-PLC γ1 has been described in OA chondrocytes, where its increase directly affects the increase of MMP-13 and the decrease of ECM components, such as aggrecan and collagen type II, thus contributing to OA progression.[53] This effect on MMP-13, aggrecan and collagen type II is mediated by mTOR/P70S6K/S6 pathway. In our experimental model, OA synoviocytes, we found a similar effect with the decrease of PI-PLC γ1 associated to the decrease of MMP-3, MMP-13, and ADAMTS-5. In our scenario, we may speculate that the PI-PLC γ1 unspliced mRNA is degraded or that the protein is synthesized, but it is nonfunctional. Both the lack of protein and the presence of truncated form are an obstacle to the activation of the pathway and thus the activation of transcription of several genes among them the MMPs.[54,55]

In conclusion, we described, for the first time, the presence of the IR phenomenon in the PI-PLC γ1 coding gene in synoviocyte cells. This phenomenon leads to the decrease of PI-PLC γ1 protein, that in turn is associated with the decrease of MMP enzymes, particularly after the treatment of cells with *H. procumbens* extract.

Further studies are needed to understand why the IR phenomenon is present in some individuals, whether the splicing machine is impaired and the HPE treatment can further affects that machine. Moreover, a consideration regarding the individual response to different treatments is mandatory. Previously, we found that all analyzed samples in response to HPE treatment decreased ERK phosphorylation/activation, even if not all samples showed a decrease of MMP-13 enzyme. Thus, the modulation of ERK phosphorylation could not be associated to the MMP-13 decrease. In the present study, we found an explanation for this result, the MMP modulation can be appreciated in samples that show the PI-PLC γ1 IR, describing for the first time an association between PI-PLC γ1 decrease and MMP modulation in synoviocytes. Interestingly, we also account for the different individual responses to nutraceutical administration. The use of nutraceuticals as part of a personalized treatment could increase the quality of life, but is necessary to evaluate individual variability to personalized medicine.

AUTHOR CONTRIBUTIONS

Alessia Mariano: Methodology; investigation; formal analysis; funding acquisition; writing—review and editing. **Sergio Ammendola**: Writing—review and editing. **Arianna Migliorini**: Computational analysis. **Martina Leopizzi**: Methodology. **Domenico Raimondo**: Computational analysis and writing—review and editing. **Anna Scotto d'Abusco**: Conceptualization; funding acquisition; writing—review and editing; resources; supervision. All authors have read and agreed to the submitted version of the manuscript.

ACKNOWLEDGMENTS

We would like to thank Dr. Mariangela Lopreaito e Dr. Roberto Mattioli for helpful discussion, and we are very grateful to them for the critical reading of the manuscript. This research was funded by Progetto Facoltà 2020, #. RP1201729DF2A57F, and Progetto Avvio alla Ricerca 2021, #. AR12117A2DCE5BF7, Sapienza University of Roma, Italy.

CONFLICT OF INTEREST STATEMENT

The authors declare no conflict of interest.

DATA AVAILABILITY STATEMENT

Data are contained within the manuscript.

ORCID

Alessia Mariano http://orcid.org/0000-0002-9569-8952
Sergio Ammendola http://orcid.org/0000-0001-9452-2456
Arianna Migliorini http://orcid.org/0009-0001-3649-6293
Martina Leopizzi http://orcid.org/0000-0002-9258-4191
Domenico Raimondo http://orcid.org/0000-0002-1780-7295
Anna Scotto d'Abusco http://orcid.org/0000-0002-3323-6015

REFERENCES

1. Grabski DF, Broseus L, Kumari B, Rekosh D, Hammarskjold ML, Ritchie W. Intron retention and its impact on gene expression and protein diversity: a review and a practical guide. *WIREs RNA*. 2021;12:e1631. doi:10.1002/wrna.1631
2. Monteuuis G, Wong JJL, Bailey CG, Schmitz U, Rasko JEJ. The changing paradigm of intron retention: regulation, ramifications and recipes. *Nucleic Acids Res*. 2019;47:11497-11513 doi:10.1093/nar/gkz1068

3. Lareau LF, Inada M, Green RE, Wengrod JC, Brenner SE. Unproductive splicing of SR genes associated with highly conserved and ultraconserved DNA elements. *Nature*. 2007;446:926-929. doi:10.1038/nature05676
4. Zheng S, Gray EE, Chawla G, Porse BT, O'Dell TJ, Black DL. PSD-95 is post-transcriptionally repressed during early neural development by PTBP1 and PTBP2. *Nature Neurosci*. 2012;15:381-388. doi:10.1038/nn.3026
5. Yap K, Lim ZQ, Khandelia P, Friedman B, Makeyev EV. Coordinated regulation of neuronal mRNA steady-state levels through developmentally controlled intron retention. *Genes Dev*. 2012;26:1209-1223. doi:10.1101/gad.188037.112
6. Kalyna M, Simpson CG, Syed NH, et al. Alternative splicing and nonsense-mediated decay modulate expression of important regulatory genes in *Arabidopsis*. *Nucleic Acids Res*. 2012;40:2454-2469. doi:10.1093/nar/gkr932
7. Kaur G, Helmer RA, Smith LA, Martinez-Zaguilan R, Dufour JM, Chilton BS. Alternative splicing of helicase-like transcription factor (Hltf): intron retention-dependent activation of immune tolerance at the feto-maternal interface. *PLoS One*. 2018;13:e0200211. doi:10.1371/journal.pone.0200211
8. Middleton R, Gao D, Thomas A, et al. IRFinder: assessing the impact of intron retention on mammalian gene expression. *Genome Biol*. 2017;18:51. doi:10.1186/s13059-017-1184-4
9. Ullrich S, Guigó R. Dynamic changes in intron retention are tightly associated with regulation of splicing factors and proliferative activity during B-cell development. *Nucleic Acids Res*. 2020;48:1327-1340. doi:10.1093/nar/gkz1180
10. Edwards CR, Ritchie W, Wong JJ-L, et al. A dynamic intron retention program in the mammalian megakaryocyte and erythrocyte lineages. *Blood*. 2016;127:e24-e34. doi:10.1182/blood-2016-01-692764
11. Memon D, Dawson K, Smowton CS, Xing W, Dive C, Miller CJ. Hypoxia-driven splicing into noncoding isoforms regulates the DNA damage response. *NPJ Genom Med*. 2016;1:16020. doi:10.1038/npjgenmed.2016.20
12. Liu Y-Z, Wang Y-X, Jiang C-L. Inflammation: the common pathway of stress-related diseases. *Front Hum Neurosci*. 2017;11:316. doi:10.3389/fnhum.2017.00316
13. Ibáñez-Costa A, Perez-Sanchez C, Patiño-Trives AM, et al. Splicing machinery is impaired in rheumatoid arthritis, associated with disease activity and modulated by anti-TNF therapy. *Ann Rheum Dis*. 2022;81:56-67. doi:10.1136/annrheumdis-2021-220308
14. Jung H, Lee D, Lee J, et al. Intron retention is a widespread mechanism of tumor-suppressor inactivation. *Nature Genet*. 2015;47:1242-1248. doi:10.1038/ng.3414
15. Scanzello CR. Role of low-grade inflammation in osteoarthritis. *Curr Opin Rheumatol*. 2017;29:79-85. doi:10.1097/BOR.0000000000000353
16. Martel-Pelletier J, Barr AJ, Cicuttini FM, et al. Osteoarthritis. *Nat Rev Dis Primers*. 2016;2:16072. doi:10.1038/nrdp.2016.72
17. Loeser RF, Goldring SR, Scanzello CR, Goldring MB. Osteoarthritis: a disease of the joint as an organ. *Arthritis Rheumatism*. 2012;64:1697-1707. doi:10.1002/art.34453
18. Mariano A, Di Sotto A, Leopizzi M, et al. Antiarthritic effects of a root extract from *Harpagophytum procumbens* DC: novel insights into the molecular mechanisms and possible bioactive phytochemicals. *Nutrients*. 2020;12:2545. doi:10.3390/nu12092545
19. Mariano A, Bigioni I, Mattioli R, et al. *Harpagophytum procumbens* root extract mediates anti-inflammatory effects in osteoarthritis synoviocytes through CB2 activation. *Pharmaceuticals*. 2022;15:457. doi:10.3390/ph15040457
20. Fais P, Leopizzi M, Di Maio V, et al. Phosphoinositide-specific phospholipase C in normal human liver and in alcohol abuse. *J Cell Biochem*. 2019;120:7907-7917. doi:10.1002/jcb.28067
21. Mirdita M, Schütze K, Moriwaki Y, Heo L, Ovchinnikov S, Steinegger M. ColabFold: making protein folding accessible to all. *Nature Methods*. 2022;19:679-682. doi:10.1038/s41592-022-01488-1
22. Goddard TD, Huang CC, Meng EC, et al. UCSF ChimeraX: meeting modern challenges in visualization and analysis. *Prot Sci*. 2018;27:14-25. doi:10.1002/pro.3235
23. Zambrano R, Jamroz M, Szczasiuk A, Pujols J, Kmiecik S, Ventura S. AGGRESCAN3D (A3D): server for prediction of aggregation properties of protein structures. *Nucleic Acids Res*. 2015;43:W306-W313. doi:10.1093/nar/gkv359
24. Hajicek N, Keith NC, Siraliev-Perez E, et al. Structural basis for the activation of PLC-γ isozymes by phosphorylation and cancer-associated mutations. *eLife*. 2019;8:e51700. doi:10.7554/eLife.51700
25. Liao H-J, Carpenter G. Phospholipase C. *Handbook of Cell Signalling*. Elsevier; 2010:887-891. doi:10.1016/B978-0-12-374145-5.00110-8
26. Nakamura Y, Fukami K. Regulation and physiological functions of mammalian phospholipase C. *J Biochem*. 2017;161:mvw094. doi:10.1093/jb/mvw094
27. A, Gresset, J, Sondek, Harden TK. The phospholipase C isozymes and their regulation. *SubCell Biochem*. 2012:61-94. doi:10.1007/978-94-007-3012-0_3
28. Haas E, Stanley DW. Phospholipase C. *xPharm The Comprehensive Pharmacology Reference*. Elsevier; 2007:1-7. doi:10.1016/B978-008055232-3.60543-4
29. Hajicek N, Charpentier TH, Rush JR, Harden TK, Sondek J. Autoinhibition and phosphorylation-induced activation of phospholipase C-γ isozymes. *Biochemistry*. 2013;52:4810-4819. doi:10.1021/bi400433b
30. Ensembl. Gene: PLCG1 ENSG00000124181, 2023. https://jul2022.archive.ensembl.org/Homo_sapiens/Gene/Summary?db=core;g=ENSG00000124181;r=20:41136960-41196801;t=ENST00000473632
31. Tao P, Han X, Wang Q, et al. A gain-of-function variation in PLCG1 causes a new immune dysregulation disease. *J Allergy Clin Immunol*. 2023;152:1292-1302. doi:10.1016/j.jaci.2023.06.020
32. Patel VM, Flanagan CE, Martins M, et al. Frequent and persistent PLCG1 mutations in sézary cells directly enhance PLCγ1 activity and stimulate NFκB, AP-1, and NFAT signaling. *J Invest Dermatol*. 2020;140:380-389.e4. doi:10.1016/j.jid.2019.07.693
33. Prawiro C, Bunney TD, Kampyli C, Yaguchi H, Katan M, Bangham CRM. A frequent PLCγ1 mutation in adult T-cell leukemia/lymphoma determines functional properties of the malignant cells. *Biochimica et Biophysica Acta (BBA)—Mol Basis Dis*. 2023;1869:166601. doi:10.1016/j.bbadis.2022.166601
34. Behjati S, Tarpey PS, Sheldon H, et al. Recurrent PTPRB and PLCG1 mutations in angiosarcoma. *Nature Genet*. 2014;46:376-379. doi:10.1038/ng.2921
35. Chen X, Chen R, Xu Y, Xia C. PLCγ1 inhibition combined with inhibition of apoptosis and necroptosis increases cartilage matrix synthesis in IL-1β-treated rat chondrocytes. *FEBS Open Bio*. 2021;11:435-445. doi:10.1002/2211-5463.13064
36. Chen L, Deng H, Cui H, et al. Inflammatory responses and inflammation-associated diseases in organs. *Oncotarget*. 2018;9:7204-7218. doi:10.18632/oncotarget.23208
37. Geczy QE, Thirumaran AJ, Carroll PR, McLachlan AJ, Hunter DJ. What is the most effective and safest non-steroidal anti-inflammatory drug for treating osteoarthritis in patients with comorbidities. *Expert Opin Drug Metab Toxicol*. 2023;19:681-695. doi:10.1080/17425255.2023.2267424
38. Apostu D, Lucaciu O, Mester A, et al. Systemic drugs with impact on osteoarthritis. *Drug Metab Rev*. 2019;51:498-523. doi:10.1080/03602532.2019.1687511
39. Mariano A, Bigioni I, Misiti F, Fattorini L, Scotto d'Abusco A, Rodio A. The nutraceuticals as modern key to achieve erythrocyte oxidative

stress fighting in osteoarthritis. *Curr Issues Mol Biol*. 2022;44:3481-3495. doi:10.3390/cimb44080240
40. Favero M, Belluzzi E, Trisolino G, et al. Inflammatory molecules produced by meniscus and synovium in early and end-stage osteoarthritis: a coculture study. *J Cell Physiol*. 2019;234:11176-11187. doi:10.1002/jcp.27766
41. Li T, Peng J, Li Q, Shu Y, Zhu P, Hao L. The mechanism and role of ADAMTS protein family in osteoarthritis. *Biomolecules*. 2022;12:959. doi:10.3390/biom12070959
42. Grillet B, Pereira RVS, Van Damme J, Abu El-Asrar A, Proost P, Opdenakker G. Matrix metalloproteinases in arthritis: towards precision medicine. *Nat Rev Rheumatol*. 2023;19:363-377. doi:10.1038/s41584-023-00966-w
43. Behrendt P, Preusse-Prange A, Klüter T, et al. IL-10 reduces apoptosis and extracellular matrix degradation after injurious compression of mature articular cartilage. *Osteoarthritis Cartilage*. 2016;24:1981-1988. doi:10.1016/j.joca.2016.06.016
44. Wan J, Zhang G, Li X, et al. Matrix metalloproteinase 3: a promoting and destabilizing factor in the pathogenesis of disease and cell differentiation. *Front Physiol*. 2021;12:663978. doi:10.3389/fphys.2021.663978
45. Tardif G, Reboul P, Pelletier J-P, Martel-Pelletier J. Ten years in the life of an enzyme: the story of the human MMP-13 (collagenase-3). *Modern Rheumatol*. 2004;14:197-204. doi:10.1007/s10165-004-0292-7
46. Simão M, Gavaia PJ, Camacho A, et al. Intracellular iron uptake is favored in Hfe-KO mouse primary chondrocytes mimicking an osteoarthritis-related phenotype. *Biofactors*. 2019;45:583-597. doi:10.1002/biof.1520
47. Scotto d'Abusco A, Calamia V, Cicione C, Grigolo B, Politi L, Scandurra R. Glucosamine affects intracellular signalling through inhibition of mitogen-activated protein kinase phosphorylation in human chondrocytes. *Arthritis Res Ther*. 2007;9:R104. doi:10.1186/ar2307
48. Goldring M, Otero M, Plumb D, et al. Roles of inflammatory and anabolic cytokines in cartilage metabolism: signals and multiple effectors converge upon MMP-13 regulation in osteoarthritis. *European Cells and Materials*. 2011;21:202-220. doi:10.22203/eCM.v021a16
49. Verma P, Dalal K. ADAMTS-4 and ADAMTS-5: key enzymes in osteoarthritis. *J Cell Biochem*. 2011;112:3507-3514. doi:10.1002/jcb.23298
50. Jiang L, Lin J, Zhao S, et al. ADAMTS5 in osteoarthritis: biological functions, regulatory network, and potential targeting therapies. *Front Mol Biosci*. 2021;8:703110. doi:10.3389/fmolb.2021.703110
51. de Almeida LGN, Thode H, Eslambolchi Y, et al. Matrix metalloproteinases: from molecular mechanisms to physiology, pathophysiology, and pharmacology. *Pharmacol Rev*. 2022;74:714-770. doi:10.1124/pharmrev.121.000349
52. Kobayashi H, Hirata M, Saito T, Itoh S, Chung U, Kawaguchi H. Transcriptional induction of ADAMTS5 protein by nuclear factor-κB (NF-κB) family member RelA/p65 in chondrocytes during osteoarthritis development. *J Biol Chem*. 2013;288:28620-28629. doi:10.1074/jbc.M113.452169
53. Zeng G, Cui X, Liu Z, et al. Disruption of phosphoinositide-specific phospholipases Cγ1 contributes to extracellular matrix synthesis of human osteoarthritis chondrocytes. *Int J Mol Sci*. 2014;15:13236-13246. doi:10.3390/ijms150813236
54. Liu Y, Bunney TD, Khosa S, et al. Structural insights and activating mutations in diverse pathologies define mechanisms of deregulation for phospholipase C gamma enzymes. *EBioMedicine*. 2020;51:102607. doi:10.1016/j.ebiom.2019.102607
55. Zheng J, Zhang W, Li L, et al. Signaling pathway and small-molecule drug discovery of FGFR: a comprehensive review. *Front Chem*. 2022;10:860985. doi:10.3389/fchem.2022.860985

SUPPORTING INFORMATION

Additional supporting information can be found online in the Supporting Information section at the end of this article.

How to cite this article: Mariano A, Ammendola S, Migliorini A, Leopizzi M, Raimondo D, Scotto d'Abusco A. Intron retention in PI-PLC γ1 mRNA as a key mechanism affecting MMP expression in human primary fibroblast-like synovial cells. *Cell Biochem Funct*. 2024;42:e4091. doi:10.1002/cbf.4091